Arch. Environ. Contam. Toxicol. 52, 47–57 (2007)
DOI: 10.1007/s00244-005-0213-6

ARCHIVES OF
Environmental
Contamination
and Toxicology

Preliminary Examination of Short-Term Cellular Toxicological Responses of the Coral *Madracis mirabilis* to Acute Irgarol 1051 Exposure

C. Downs,[1] A. Downs[2]

[1] Haereticus Environmental Laboratory, P.O. Box 93, Clifford, VA 24533, USA
[2] Department of Molecular, Cellular, and Developmental Biology, Yale University, 266 Whitney Avenue, New Haven, CT 06511, USA

Received: 23 August 2005 / Accepted: 4 April 2006

Abstract. Irgarol 1051 is an *s*-triazine herbicide formulated with Cu2O in antifouling paints. Recent studies have shown that Irgarol 1051 inhibits coral photosynthesis at environmentally relevant concentrations, consistent with its mode of action as a photosystem II inhibitor. Related toxicologic effects of this herbicide on coral cellular physiology have not yet been investigated. We used cellular diagnostics to measure changes in 18 toxicologic cellular parameters in endosymbiotic algal (dinoflagellate) and cnidarian (host) fractions of the common branching coral *Madracis mirabilis* associated with *in vivo* 8- and 24-hour exposures to a nominal initial Irgarol 1051 concentration of 10 μg L^{-1}. Responses measured were (1) xenobiotic response, which includes total and dinoflagellate multixenobiotic resistance (MXR), cnidarian cytochrome (CYP) P450−3 and P450-6 classes, cnidarian, and dinoflagellate glutathione-s-transferase (GST); (b) oxidative damage and response, which includes cnidarian and dinoflagellate Cu/Zn and Mn superoxide dismutase (SOD), cnidarian and dinoflagellate glutathione peroxidase (GPx), cnidarian catalase, and total protein carbonyl); (3) metabolic homeostasis, which includes chloroplast and invertebrate small heat-shock proteins (sHsp), cnidarian protoporphyrinogen oxidase IX (PPO), cnidarian ferrochelatase, and cnidarian heme oxygenase; and (4*)* protein metabolic condition, which includes cnidarian and dinoflagellate heat shock proteins (hsp70 and hsp60), total ubiquitin, and cnidarian ubiquitin ligase. Acute responses to Irgarol 1051 exposure included significant increases in total and dinoflagellate MXR, dinoflagellate Cu/Zn SOD, dinoflagellate chloroplast sHsp, and cnidarian PPO. Irgarol 1051 exposure resulted in decreases in cnidarian GPx, cnidarian ferrochelatase, cnidarian catalase, and cnidarian CYP 450-3 and -6 classes. Related implications of Irgarol 1051 exposure to coral cellular condition are discussed.

Contamination by the antifouling *s*-triazine herbicide Irgarol 1051 (*N*'-tert-butyl-*N*-cyclopropyl-6-(methylthio)-1,3,5-triazine-2,4-diamine) in temperate and tropical marine ecosystems is increasing (Konstantinou & Albanis 2004). Irgarol 1051's principle action of toxicity for algae and plants is as a photosystem II inhibitor; Irgarol competes for the Q_B-binding site of the chlorophyll D1 protein, inhibiting the chloroplast-electron transport chain (Hall *et al.* 1999). A number of studies have shown that Irgarol 1051 inhibits photosynthesis of both isolated endosymbiotic algae (*i.e.*, dinoflagellate *in vitro*) and intact symbiosis (*i.e.*, whole coral *in vivo*) in a number of coral species and was observed to exhibit comparatively higher toxicity compared with other triazine and nontriazine herbicides (Owen *et al.* 2002; Owen *et al.* 2003; Jones *et al.* 2003). Acute photosynthetic inhibition was observed at low concentrations of this antifoulant (≥0.05 μg L^{-1}; Owen *et al.* 2003). The range of environmental concentrations that have been reported in the literature are typically between undetectable and 0.7 μg L^{-1}, although values in the range of 1.7 to 4 μg L^{-1} have been occasionally reported in areas of high boating activity (Readman *et al.* 1993; Basheer *et al.* 2002; Hall *et al.* 2004). These findings should be assessed in the context that corals represent structurally and functionally critical components of reef ecosystems and are the major primary producers in these environments.

Although the impacts on coral photosynthesis of acute low-level exposure to Irgarol 1051 have been shown, other potential toxicity mechanisms associated with exposure to this antifoulant in cnidaria have not been investigated (Dhal & Blank 1996). To this end, we applied the approach of cellular diagnostics (Downs *et al.* 2000; Brown *et al.* 2002a; Downs *et al.* 2002; Downs 2005) to identify mechanisms of toxicity and stress in the common branching coral *Madracis mirabilis* resulting from acute (24-hour) *in vivo* Irgarol 1051 exposure (10 μg L^{-1}). The cellular diagnostic method measures changes in cellular end points that reflect changes in structural and functional cellular pathways, which when used appropriately may enable (1) an assessment of cellular-physiologic condition of an individual or population, (2) identification of putative stressors either by direct measurement of the stressor or by profiling stressor-specific effects, and (3) forecasting higher-order behavior based on an understanding of cellular-level processes (Downs 2005). Application of the cellular diagnostic method assesses both changes in the cellular ''health'' of the organism and mechanisms of toxicity associated with Irgarol 1051 exposure.

Correspondence to: C. Downs; *email:* cadowns@gmail.com

Methods

Reagents

All chemicals for buffered solutions were obtained from EM Science (Gibbstown, NJ). Polyvinylidene fluoride (PVDF) membrane was obtained from Millipore (Bedford, MA). Antibodies and calibration standards were obtained from EnVirtue Biotechnologies (Winchester, VA). Antirabbit conjugated horseradish peroxidase antibodies were obtained from Jackson Immunoresearch (West Grove, PA).

Irgarol 1051 Coral Exposures

Colonies of the branching coral *Madracis mirabilis* were collected from the coastal waters of Bermuda and acclimated in an indoor raceway under natural sunlight (peak irradiance approximately 300 µmol photosynthetic active radiation/m/sec). The raceway was fed continuous fresh, unfiltered seawater for 3 months before use. Corals appeared in good health, with no visible signs of bleaching at the start of the experiment.

Seawater for the experiments was collected at an offshore site 1.5 miles from the coast of Bermuda, 30 cm below the surface, and was 0.2-µm filtered to remove microalgae (Owen *et al.* 2002). Solid-phase extraction of a 2-L sample and subsequent gas chromatography–mass spectrometry analysis (Owen *et al.* 2002) confirmed that the Irgarol 1051 in the water used in the experiment was below the limit of detection (2 ng L^{-1}).

Single coral branches (approximately 1 cm diameter × 3 to 4 cm length) were detached from several coral colonies by carefully cutting across the base of the branch, handling and cutting well below the line of living tissue to avoid physical contact and stress to the coral. Immediately after detachment, a single branch was transferred to 1 of 20 1-liter glass beakers (prepared by washing once in 10% HCl, three times in acetone, and a final rinse in Milli-Q water). All preparation of coral branches was done underwater to prevent contact with air. Each coral branch was held vertically in the beaker by placing its base into a cleaned 1 cm^2 plastic grating fixed to the beaker's base. Plastic grating presents a caveat to this study because of the adhesion coefficient of Irgarol and its breakdown products to plastic, thereby confounding the calculated exposure concentration of the coral to Irgarol. Unfortunately, the plastic grating was used because it was the only material available at the time of the study that could keep this branching coral upright. Beakers containing a coral branch in 1 L seawater were randomly assigned to four treatments with n = 5/treatment; treatment 1 = control for 8 hours; treatment 2 = exposure to a nominal initial concentration of 10 µg L^{-1} Irgarol 1051 for 8 hours; treatment 3 = control for 24 hours; treatment 4 = exposure to a nominal initial concentration of 10 µg L^{-1} Irgarol 1051 for 24 hours. A 1 mg mL^{-1} Irgarol 1051 standard was made up in high-pressure liquid chromatography–grade acetone, and 10 µl was added to each beaker in treatments 2 and 4, and 10 µL acetone was added to treatments 1 and 3 (controls) to account for any solvent effects. Beakers were individually aerated by way of sterile 12-gauge syringe needle.

The experiment was begun at 8:00 AM in the morning and conducted in a covered outside raceway under a natural 12-hour light/12-hour dark photoperiod. Beakers stood in running seawater to maintain temperature stability. Neutral density filter and shading were used to decrease peak light levels to approximately 600 µmol photosynthetic active radiation/m/sec. The temperature of the water in the dosing containers ranged from 22°C to 25°C through the exposure.

For the 24-hour exposure treatments, after 12 hours of exposure, coral branches were transferred to new beakers with clean water and spiked with Irgarol 1051 or solvent as previously described. Gloves were exchanged after transfer of each coral. At the end of the exposure, each coral branch was gently patted dry with article towel to remove excess coral mucus and seawater. Using gloved hands and sterile (autoclaved) calipers, the top tip section of each coral branch was removed (approximately 1 cm^2), placed in a sterile cryovial, and immediately stored at −80°C. The process of removing each coral branch and transfer to −80°C took <2 minutes.

Sample Preparation, Enzyme-Linked Immunosorbent Assay Validation, and Enzyme-Linked Immunosorbent Assay

Coral samples were ground to a powder with a liquid nitrogen–chilled ceramic pestle and mortar. Samples (approximately 10 mg) of frozen tissue were placed in 1.8-mL microcentrifuge tubes along with 1.4 mL denaturing buffer consisting of 2% sodium dodecyl sulfate (SDS), 50 mM Tris-HCl (pH 7.8), 15 mM dithiothreitol, 10 mM ethylene diamine tetraacetic acid, 0.5 mM desferoximine methylate, 0.001 mM sorbitol, 7% polyvinylpolypyrrolidone (weight/volume [wt/vol]), 0.01% polyvinylpyrrolidone (wt/vol), 0.005 mM salicylic acid, 0.01 mM 4-(2-aminoethyl)-benezensulfonyl fluoride, 0.04 mM Bestatin, 0.001 E-64, 2 mM phenylmethylsulfonyl fluoride, 2 mM benzamidine, 0.01 mM apoprotin, 5 µM a-amino-caproic acid, and 1 µg/100 uL pepstatin A. Samples were heated at 92°C for 3 minutes, vortexed for 20 seconds, incubated at 92°C for another 3 minutes, and then incubated at 25°C for 5 minutes. Samples were centrifuged at 10,000 g for 10 minutes. Supernatant free of a lipid/glycoprotein mucilage matrix was transferred to a new tube, centrifuged at 10,000 g for 5 minutes, again transferred to a new tube, and subjected to protein concentration assay (Ghosh *et al.* 1988).

Antigens to antibodies were designed from conserved, but unique, domains from unpublished cDNA sequences from various coral species and published sequences from other invertebrate species, such as bivalves and arthropods. The same strategy was used for the dinoflagellate-specific antibodies, but instead, published genomic, cDNA, and Expressed Sequence Tags (EST) sequences from GenBank were used to determine conserved domains. Antibodies were increased against an 8- to 12-residue polypeptide conjugated to oval albumin. Antigens were designed based on extremely conserved and unique domains found within the target protein. All antibodies used in this study were immunopurified with a Pierce SulfoLink Kit (catalogue no. 44895, Pierce Biotechnology, Rockford, IL, USA) using the original unconjugated peptide as the affinity-binding agent.

One-dimensional SDS–polyacrylamide gel electrophoresis (PAGE) and Western blotting validated the legitimacy of enzyme-linked immunosorbent assay (ELISA) on this species of coral using a specific antibody (Downs 2005). Five to 15 µg total soluble protein of coral supernatant was loaded onto an 8-cm SDS polyacrylamide gel with various concentrations of bis/acrylamide. A Tris [2-carboxyethyl] phosphine (TCEP) concentration of 1 mM was added to gels loaded with samples to be assayed along with antibody to the chloroplast sHsp and invertebrate sHsp. TCEP is a thiol-decreasing agent that will not migrate through a gel when the gel is subjected to an electric field. Gels were blotted onto PVDF membrane using a wet-transfer system. Membranes were blocked in 7% nonfat dry milk and incubated with the primary antibody for 1 hour. The blots were washed in Tris-buffered saline (TBS) four times and incubated in a horseradish peroxidase–conjugated secondary antibody solution for 1 hour. Blots were washed four times in TBS and developed using NEN Western Lightning Plus luminol/hydrogen peroxide–based chemiluminescent solution and documented using a Syngene Genegnome luminescent documentation system.

Once validated, antibodies and samples were optimized and precision determined for ELISA using an 8 × 6 × 4 factorial design (Crowther 1999). A Beckman-Coulter Biomek 2000 with 384-well microplates was used to conduct the ELISA assays. Samples were assayed according to EnVirtue Biotechnologies' antibodies (generated

in rabbits): antialgal glutathione peroxidase (AB-G101-P), antialgal manganese superoxide dismutase (SOD) (AB-S100-P), antialgal Cu/Zn SOD (AB-101-PA), antialgal heat-shock protein (Hsp) 60 (AB-H100-P), antialgal Hsp 70 (AB-H101-P), antialgal glutathione-s-transferase, antichloroplast small Hsp (AB-H104-C), antiubiquitin (AB-U100), anticnidarian Hsp 70 (AB-H101-CDN), anticnidarian Hsp 60 (AB-H100-IN), anticnidarian manganese SOD (AB-S100-MM), anticnidarian Cu/Zn SOD (cytosolic isoform, lot 1517), anticnidarian glutathione peroxidase, anticnidarian glutathione-s-transferase (alpha-isoform homologue), anti-invertebrate small Hsp (AB-H103), anticnidarian ferrochelatase (lot 1939), anticnidarian heme-catalase (cytosolic homologue, lot 3113), anticnidarian protoporphyrinogen oxidase IX (lot 1945), anticnidarian heme oxygenase I (lot 3114), anticnidarian cytochrome P450-3 class (lot 1986), anticnidarian ubiquitin ligase E2 (lot 3109), anticnidarian cytochrome P450-6 class (lot 1984), and anti-MXR (ABC family of proteins; P-glycoprotein 140 and 160; AB-MDR-160). All antibodies are monospecific polyclonal antibodies made against a synthetic eight–amino-acid residue polypeptide that reflects a specific region of the target protein. Protein carbonyl was assayed using the method described in Downs *et al.* (2002). Samples were assayed in triplicate with intraspecific variation (%CV) of < 6% for each assay. An eight-point calibrant curve, using a calibrant relevant to each antibody, was plated in triplicate for each plate. Calibrants for each ELISA contained the unconjugated peptide used to produce the antibody. Formula weight and molarity are known for each calibrant; hence, final units can be calculated for the number of moles of antigen/target protein/measure total soluble protein.

Statistical Analysis

Planned (*a priori*) and unplanned (*a posteriori* or *post hoc)* comparison tests were used depending on whether the question posed for a specific data set contained fundamental hypotheses, as in the case of a quantitative diagnostic strategy (Downs 2005). Data were tested for normality using Kolmogorov-Smirnov test (with Lilliefors' correction) and for equal variance using Levene Median test. If data were normally distributed and homogeneous, unpaired Student *t* test with $\alpha = 0.05$ was employed. When data did not meet normality and equal variance assumptions, we employed Mann-Whitney Rank Sum test (Sokal & Rohlf 1995).

We used canonical correlation analysis (CCA) as a heuristic tool to illustrate how biomarkers could be used to discriminate among environmental stressors. CCA is an Eigen analysis method that reveals the basic relationships between two matrices (Gauch 1985); in our case, those of the four treatments and biomarker data. CCA provided an objective statistical tool to (1) determining if treatments were different from one another using biomarkers indicative of a cellular process (*e.g.*, protein metabolic condition, xenobiotic response) and (2) determine which biomarkers contributed to those differences. This analysis required combining data from all four treatments into one matrix, which we did by expressing biomarker responses in a given treatment as a proportion of their mean level in the control. The experimental design was constrained by two assumptions of the CCA, *i.e.*, that stressor gradients were independent and linear.

Results and Discussion

Antibody Validation

Antibodies against cnidarian and dinoflagellate cellular parameters did not exhibit significant nonspecific cross-reactivity (Figs. 1 through 4); hence, they could be validly used in an ELISA format. Because of the evolutionary conservation of ubiquitin and MXR, these antibodies detected proteins from both dinoflagellate and cnidarian species in the coral homogenate (Fig. 3; ubiquitin data not shown); consequently, an ELISA measurement using this antibody detects total concentration for these proteins. In MXR-dinoflagellate, the antibody against this protein is specific for a conserved domain of the homologue of ABC proteins found only in plant/algae in plants. This was determined by way of SDS-PAGE/Western separation and analysis of two purified samples, pure *Symbiodinium ssp.* and a coral homogenate lacking *Symobiodinium.* Algae and plants have multiple isoforms of GST-theta (Ketter 2001; Dixon *et al.* 2002); hence, the multiple banding pattern seen in Figure 4C.

ELISA Results

ELISA results are divided into the following cellular diagnostic categories: (1) protein metabolic condition, which includes dinoflagellate hsp60, dinoflagellate hsp70, cnidarian hsp60, cnidarian hsp70, cnidarian ubiquitin ligase E2, and total ubiquitin (Table 1. Cellular diagnostic markers); (2) oxidative stress and response, which includes dinoflagellate MnSOD, dinoflagellate Cu/ZnSOD, dinoflagellate GPx, cnidarian MnSOD, cnidarian Cu/ZnSOD, cnidarian GPx, cnidarian cytosolic heme-catalase, and protein carbonyl (Table 1); (3) metabolic condition, which includes cnidarian ferrochelatase, cnidarian protoporphyrinogen oxidase IX, cnidarian heme oxygenase (type 1), chloroplast sHsp, plant cytosolic sHsps classes I and II, and the four major cnidarian sHsp classes (Table 1); and (4) xenobiotic response, which includes dinoflagellate GST, cnidarian GST, cnidarian cytochrome P450-3 class, cnidarian cytochrome P450-6 class, MXR for both dinoflagellate and cnidarian MXR, and dinoflagellate-specific MXR homologue (Table 1).

The results in Tables 1 through 4 in total show that 24-hour exposure to 10 $\mu g l^{-1}$ Irgarol 1051 challenges both host (cnidarian) and symbiont (dinoflagellate) cellular homeostasis and induces stress responses in the symbiosis. These responses first serve to decrease the cellular burden of Irgarol 1051 within the symbiosis (upregulation of total and dinoflagellate cell membrane MXR [p glycoprotein]; Table 1). Antioxidant defences against an oxidative-stress-based mechanism of toxicity are also induced in the dinoflagellate but not the cnidarian fractions of the symbiosis (increases in dinoflagellate Cu/Zn SOD; Table 1). Oxidative damage after a 24-hour exposure to Irgarol 1051 is evident (production of protein carbonyl; Table 1). However, Irgarol 1051 exposure also induces subcellular perturbation of metabolic homeostasis (Table 1), which appears to mask some predicted xenobiotic detoxification and oxidative stress responses and compromise the capacity of the symbiosis to transform and detoxify xenobiotics and decrease cellular free radical burden (*e.g.*, catalase, CYP-3 and -6 classes). Decreases in ferrochelatase and increases in PPO and heme oxygenase (Table 1) suggest adverse impacts on porphyrin synthesis, damage to porphyrins, and increased porphyrin degradation. This interpretation is supported by the severe deterioration of the levels of porphyrin-dependent enzymes, such as cnidarian catalase and cnidarian CYP 450-3 and -6 classes. Least affected by Irgarol 1051 exposure was

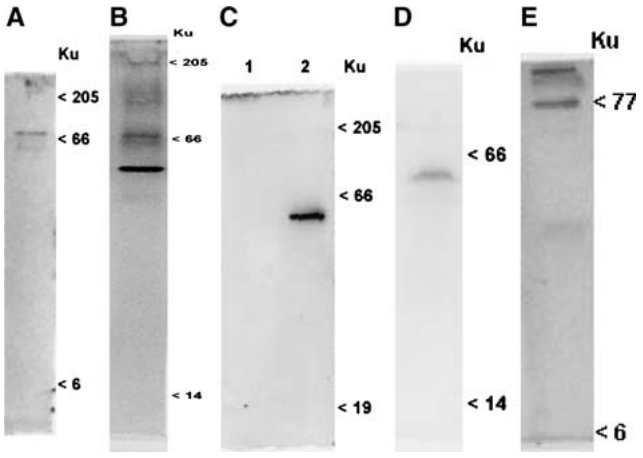

Fig. 1. Protein metabolic condition parameters. Coral were homogenized and subjected to SDS-PAGE (5 μg total soluble protein/lane) and Western blotting and assayed with polyclonal antibody against the following parameters: A = Hsp70 cnidarian; B = Hsp70 dinoflagellate; C = Hsp60 cnidarian, lane 1 = isolated dinoflagellate, lane 2 = whole-coral homogenate; D = Hsp60 dinoflagellate; E = ubiquitin ligase E2 cnidarian

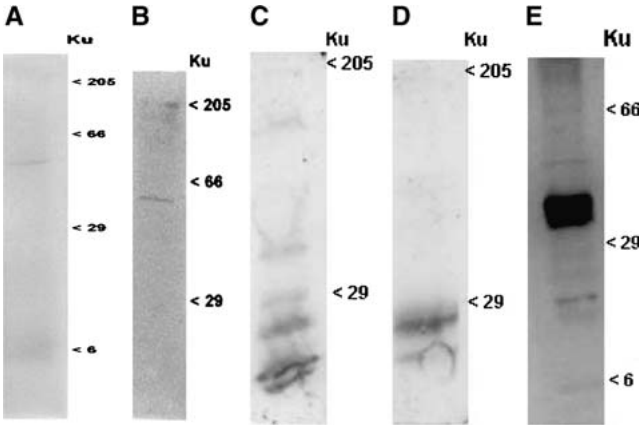

Fig. 3. Metabolic condition parameters. Coral were homogenized and subjected to SDS-PAGE (5 μg total soluble protein/lane) and Western blotting and assayed with polyclonal antibody against the following parameters: A = ferrochelatase cnidarian; B = protoporphyrinogen oxidase IX cnidarian; C = cnidarian small Hsps isoforms I through IV; D = chloroplast sHsp; E = heme oxygenase 1 cnidarian

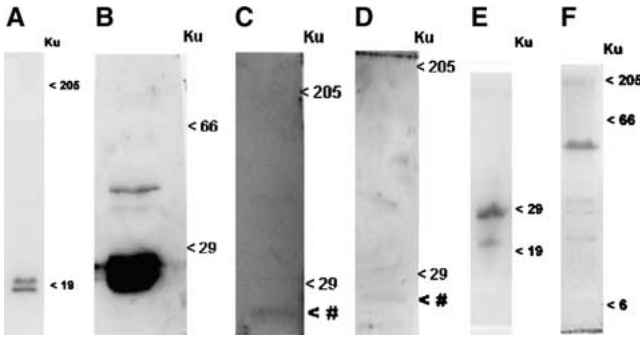

Fig. 2. Oxidative stress parameters. Coral were homogenized and subjected to SDS-PAGE (5 μg total soluble protein/lane) and Western blotting and assayed with polyclonal antibody against the following parameters: A = Cu/ZnSOD cnidarian; B = Cu/ZnSOD dinoflagellate; C = MnSOD cnidarian; D = GPx cnidarian; E = GPx dinoflagellate; F = catalase cnidarian. #Presence of appropriate migrating band

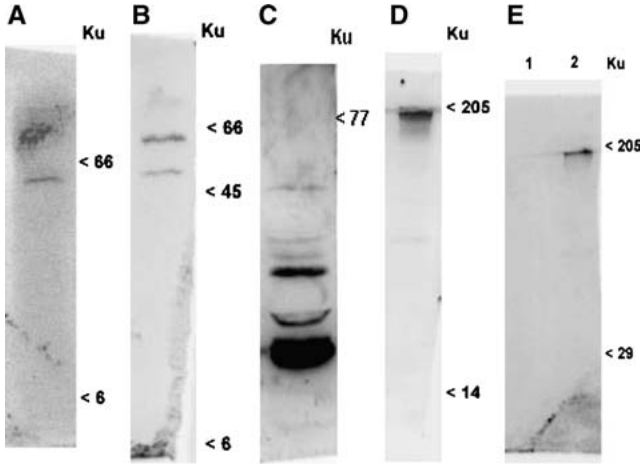

Fig. 4. Xenobiotic response parameters. Coral were homogenized and subjected to SDS-PAGE (5 μg total soluble protein/lane) and Western blotting and assayed with polyclonal antibody against the following parameters: A = cytochrome P450-3 class cnidarian; B = cytochrome P450-6 class cnidarian; C = GST dinoflagellate; D = MXR, both cnidarian and dinoflagellate isoforms; E = dinoflagellate MXR; lane 1 = coral cell suspension with the zooxanthallae spun out; lane 2 = purified *Madracis* dinoflagellate

protein metabolic condition (Table 1), with only small (and in most cases nonsignificant) effects on hsp60, hsp70, ubiquitin, and ubiquitin ligase, although the data and the statistical analysis must be interpreted cautiously (see below). We discuss the responses of biomarkers within each cellular diagnosis category in more detail below.

Protein Metabolic Condition

The equilibrium protein metabolic condition was not significantly shifted by Irgarol 1051 exposure (Table 1). A lack of consistency in the biomarker profiles in this category prevented any meaningful discrimination or diagnosis for this category between the control and Irgarol 1051 treatment groups. Part of the lack of significance between control and treatments is attributable to high within-treatment variance. It is interesting to note that the 8-hour Irgarol 1051 exposure caused a significant decrease in ubiquitin ligase levels compared with controls.

Ubiquitin ligase catalyses the second enzymatic step in conjugating ubiquitin to the target protein. Increasing levels of this protein usually indicate an increased demand for protein degradation. Decreasing levels of this protein suggest that ubiquitin-associated protein degradation rates have decreased. From our investigation of the literature, there is no precedent for an environmentally related xenobiotic-induced decrease, although targeted inhibition of ubiquitin ligase activity is a focal point of pharmacologic research concern-

Table 1. Cellular diagnostic markers

Cellular parameter	Control 8 hour	Irgarol 8 hour	Difference	Control 24 hour	Irgarol 24 hour	Difference
Hsp70 (*cnidarian*) fmol/ng TSP	67 ± 10	63 ± 17	No	80 ± 13	135 ± 13	($p = 0.018$)
Hsp70 (*zooxanthallae*) fmol/ng TSP	103 ± 14	153 ± 4	($p = 0.009$)	136 ± 28	190 ± 4	No
Hsp60 (*cnidarian*) fmol/ng TSP	70 ± 47	81 ± 38	No	83 ± 8	92 ± 5	No
Hsp60 (*zooxanthallae*) fmol/ng TSP	393 ± 55	518 ± 38	No	356 ± 58	425 ± 53	No
Ubiquitin (total) fmol/ng TSP	520 ± 69	601 ± 98	No	559 ± 37	689 ± 104	No
Ubiquitin ligase (*cnidarian*) fmol/ng TSP	1.2 ± 0.1	0.6 ± 0.1	($p = 0.012$)	0.8 ± 0.2	0.5 ± 0.0	No
Cu/Zn SOD (*cnidarian*) fmol/ng TSP	33 ± 3.0	26 ± 3.7	No	26 ± 3.6	23 ± 2.7	No
Cu/Zn SOD (*zooxanthallae*) pmol/ng TSP	0.897 ± 0.04	2.12 ± 0.42	($p = 0.008$)	0.961 ± 0.2	1.882 ± 0.2	($p = 0.027$)
Mn SOD (*cnidarian*) fmol/ng TSP	21 ± 2.9	14 ± 1.4	No	13.2 ± 1.9	11.9 ± 2.2	No
Mn SOD (*zooxanthallae*) fmol/ng TSP	5.3 ± 0.2	5.7 ± 1.0	No	6.2 ± 0.6	5.3 ± 0.5	No
GPx (*cnidarian*) fmol/ng TSP	12.3 ± 1.2	5.6 ± 0.6	($p = 0.001$)	11.6 ± 1.0	4.3 ± 0.7	($p = 0.002$)
GPx (*zooxanthallae*) fmol/ng TSP	6.4 ± 0.9	4.6 ± 2.4	No	7.2 ± 2.2	6.6 ± 1.0	No
Catalase (*cnidarian*) fmol/ng TSP	5.4 ± 3.1	0.65 ± 0.3	($p = 0.008$)	4.6 ± 0.7	0.13 ± 0.1	($p = 0.008$)
Protein carbonyl (total) nmol/ng TSP	4 ± 0.9	26.8 ± 10	No	8.4 ± 1.5	23 ± 4.7	($p = 0.021$)
Ferrochelatase (*cnidarian*) fmol/ng TSP	62 ± 17	17 ± 72.0	($p = 0.008$)	28 ± 11	9 ± 1	($p = 0.032$)
PPO (*cnidarian*) fmol/ng TSP	35 ± 5.2	116 ± 0.18	($p = 0.008$)	74 ± 8.0	128 ± 20	($p = 0.037$)
Plant cytosolic small Hsp relative units/ng TSP	0.03 ± 0.0	0.02 ± 0.0	No	0.02 ± 0.0	0.02 ± 0.0	No
Chloroplast small Hsp relative units/ng TSP	0.05 ± 0.0	0.48 ± 0.01	($p = 0.008$)	0.07 ± 0.0	0.55 ± 0.03	($p = 0.008$)
Invert small Hsps (total) relative uniting TSP	0.3 ± 0.012	0.359 ± 0.015	($p = 0.016$)	0.316 ± 0.01	0.310 ± 0.0	No
Heme oxygenase 1 (*cnidarian*) fmol/ng TSP	12 ± 2	53 ± 6	($p < 0.001$)	20 ± 0.1	57 ± 4	($p < 0.001$)
CYP P450 3-class (*cnid*) fmol/ng TSP	51 ± 5	147 ± 3	($p = 0.001$)	54 ± 7	3.7 ± 0.1	($p = 0.008$)
CYPP450 6-class (*cnid*) fmol/ng TSP	44 ± 21	11 ± 6	No	16 ± 6	0.097 ± 0.07	($p = 0.008$)
GST (*cnidarian*) pmol/ng TSP	136 ± 40	102 ± 32	No	84 ± 14	80 ± 16	No
GST (*zooxanthallae*) pmol/ng TSP	9.5 ± 0.7	7.5 ± 0.7	No	10.9 ± 2.1	6.8 ± 0.7	No
MXR (total) relative units/ng TSP	0.061 ± 0.01	0.148 ± 0.02	($p = 0.016$)	0.032 ± 0.0	0.246 ± 0.08	($p = 0.032$)
MXR (*zooxanthallae*) relative units/ng TSP	0.004 ± 0.002	0.021 ± 0.004	($p = 0.003$)	0.01 ± 0.002	0.0462 ± 0.005	($p < 0.001$)

Total soluble protein (TSP) = 0

ing a promising new strategy for cancer treatment (Adams 2004). One hypothesis is that the nucleophillic methylthio group in Irgarol 1051 can act as an active group or can be modified (oxidized to form a sulfoxide) (Raynor 1999) and act as an inhibitor of this enzyme (Hersko *et al.* 1986). Several *in vitro* enzymologic systems using either a yeast or rabbit reticulocyte platform can be used to test the presence of kinetic inhibition properties of Irgarol 1051 on ubiquitin ligase E2 activity (Berleth & Pickart 1996). Inclusion of protein carbonyl formations in the analysis of this subcellular category indicates that Irgarol 1051 exposure caused a significant increase in protein oxidative damage at least by 24 hours of exposure. An alternative hypothesis is that ubiquitin ligase may be susceptible to protein oxidative lesions, and such oxidation can result in inhibition or degradation of this protein (Ding *et al.* 2003).

Canonical component plot analysis using only cnidarian biomarkers of protein metabolic condition confirmed that there was no significant difference in biomarker patterns except for the 24-hour Irgarol 1051 treatment (Fig. 5). Overlapping centroid spheres indicate that patterns between the 8-hour control, the 24-hour control, and the 8-hour Irgarol 1051 treatments for these specific biomarkers are not significantly different. Conversely, when spheres do not overlap, a difference in the biomarker pattern between treatments is suggested. The biplot rays that radiate from the grand mean show the directions of the original biomarker responses in canonical space. Rays that move in the direction toward a sphere denote the contribution of that biomarker in affecting the position of the centroid in the plot model.

Oxidative Damage and Response

For the cnidarian host, Irgarol 1051 exposure resulted in a decrease in protein levels of two of the four antioxidant enzymes, cnidarian catalase and cnidarian GPx, which significantly decreased for both Irgarol 1051 treatments (Table 1). There was no change in either cnidarian Cu/Zn SOD or cnidarian Mn SOD. Dinoflagellate Mn SOD, such as the cnidarian counterpart, did not change. There was no change in the cnidarian Cu/Zn SOD, the cnidarian Mn SOD, or the dinoflagellate Mn SOD. Unlike the cnidarian host, there was no change in dinoflagellate Gpx. Glutathione peroxidase is a selenocysteine protein that will scavenge hydroxyl radicals and peroxides by catalysing a reaction with decreased glutathione. The isoform of catalase assayed in this study is a heme-based protein that catalyses the conversion of two molecules of hydrogen peroxide into two molecules of water and one molecule of divalent oxygen (Chelikani *et al.* 2004). The decrease in the levels of both these proteins suggests that the cnidarian cell will be much more susceptible to oxidative damage. Neither the cnidarian cytosolic Cu/Zn SOD protein level nor cnidarian Mn SOD protein levels were significantly affected (Table 1). This suggests that (1) there was no increase in intracellular superoxide concentrations within the cnidarian fraction of the symbiosis, (2) the cell was unable to generate more SOD proteins because of some effect of Irgarol 1051, or (3) any increase in superoxide was not enough to damage the SOD proteins available. Total protein carbonyl formation increased in response to Irgarol 1051 exposure, indicating that exposure induces oxidative damage, either by increasing the

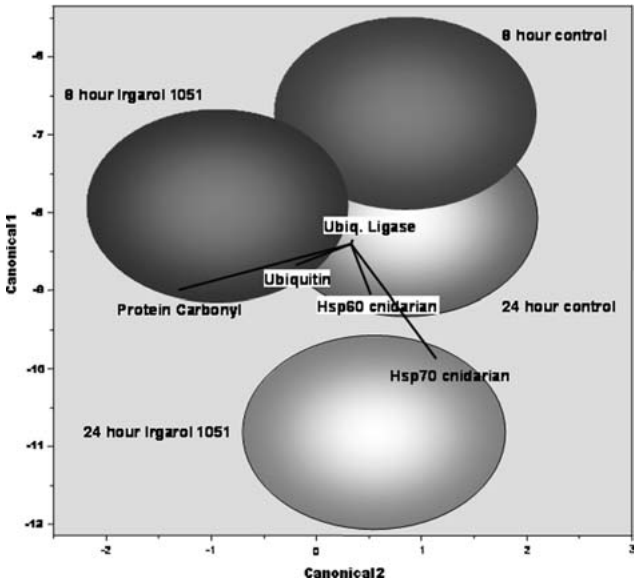

Fig. 5. Canonical centroid plot of cnidarian protein metabolic condition biomarkers. Original variates were biomarker levels expressed as a percentage of the control value in each treatment. Circles show the 95% confidence intervals about distribution centroid of each stressor. Biplot rays radiating from the grand mean show directions of original biomarker responses in canonical space. Overlapping centroids indicate that those populations are not significantly different from one another, whereas nonoverlapping centroids indicate a difference

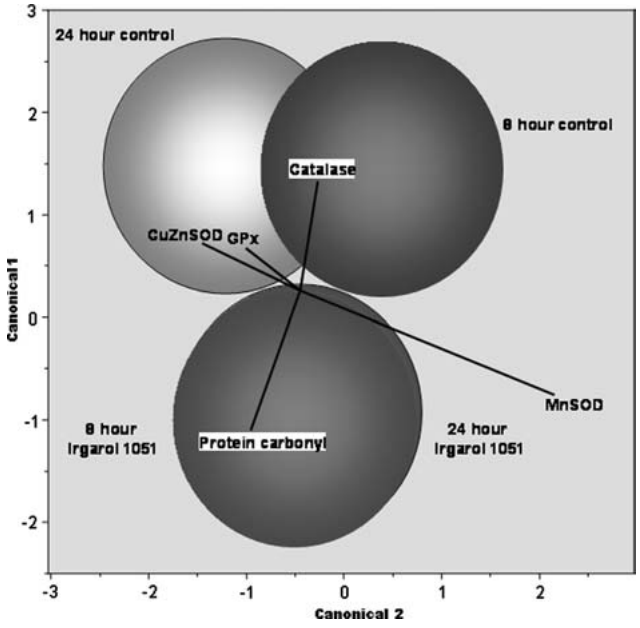

Fig. 6. Canonical centroid plot of cnidarian oxidative stress biomarkers. Original variates were biomarker levels expressed as a percentage of the control value in each treatment. Circles show the 95% confidence intervals about the distribution centroid of each stressor. Biplot rays radiating from the grand mean show directions of original biomarker responses in canonical space. Overlapping centroids indicate that those populations are not significantly different from one another, whereas nonoverlapping centroids indicate a difference

generation of reactive oxygen species, decreasing anti-oxidant defences, or both. Canonical correlation analysis of cnidarian oxidative damage and defence biomarker profiles show significant differences between both Irgarol 1051 treatments and their respective controls (Fig. 6).

The severe impact of Irgarol 1051 on cnidarian catalase is the most striking effect (Table 1). Within 8 hours of exposure to Irgarol 1051, catalase levels decreased by during 90%, and after 24 hours of exposure to Irgarol 1051, they decreased by approximately 95%. Catalase is the principal enzyme that catalyses hydrogen peroxide into water and oxygen. Two independent but synergistic mechanisms may explain this decrease in catalase protein levels. One mechanism of inhibition is based on the fact that catalase is a porphyrin-dependent enzyme whose accumulation and activity is known to decrease as a result of porphyrin synthesis interference (Haeger-Aronsen 1964; Teschke *et al.* 1983). A significant decrease in ferrochelatase would potentially result in a decrease in the available pool of porphyrins (see below), and a decrease in catalase levels is consistent with a decrease in porphyrin availability. A second possibility for the decrease in catalase levels is the extreme susceptibility of catalase to oxidation and inhibition by both singlet oxygen and superoxide (Shimizu *et al.* 1984; Lledias *et al.* 1998). Oxidation of catalase would be expected, especially in light of the increased protein carbonyl formation as a result of Irgarol 1051 exposure.

Regardless of the mechanism, a decrease in catalase has direct pathologic implications for the symbiosis. Catalase constitutes a primary defence against hydrogen peroxide generated by the zooxanthallae that would enter into the host cell through diffusion (Downs *et al.* 2002). Loss of this enzyme would leave the host cell extremely susceptible to oxidative stress and as a result may also make the symbiosis potentially more susceptible to coral bleaching (Downs *et al.* 2002).

In contrast to the cnidarian antioxidant biomarker profiles, the dinoflagellate exhibited an increase in Cu/Zn SOD levels. The antibody used in this assay was designed to specifically bind to the chloroplast Cu/Zn SOD, but it also cross-reacts with a cytosolic homologue (Wu *et al.* 1999). Both isoforms increased in response to Irgarol 1051 exposure. Regulation of the promoters for both these genes is uncharacterised, so we are unable to discriminate whether upregulation of these superoxide dismutases occurs in response to specific superoxide accumulation in the chloroplast, in the cytosol, or in both locations. Irgarol 1051 exerts its principal mode of toxicity by way of inhibition of the Q_B-binding site of photosystem II, a process that will result in the generation of photo-oxidative stress (Hall *et al.* 1999). Significant accumulation of the dinoflagellate Cu/Zn SOD supports this: Further confirmation could be obtained by exposure of corals to Irgarol 1051, isolation of the dinoflagellate from the exposed coral, and immunohistology analysis localizing oxidative damage lesions as well as gross cellular morphologic changes in the chloroplast.

Dinoflagellate Mn SOD was unaffected by Irgarol 1051 exposure, suggesting that this herbicide does not exacerbate superoxide generation in the dinoflagellate mitochondria (Wu *et al.* 1999). Canonical correlation analysis of dinoflagellate oxidative damage and defence biomarker profiles showed only a significant difference between the 8-hour control treatment and the 8-hour Irgarol 1051 exposure treatment (Fig. 7).

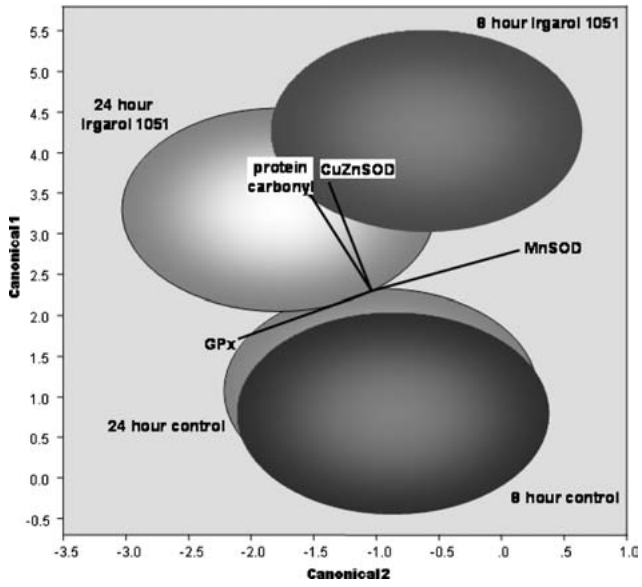

Fig. 7. Canonical centroid plot of dinoflagellate oxidative stress biomarkers. Original variates were biomarker levels expressed as a percentage of the control value in each treatment. Circles show the 95% confidence intervals about the distribution centroid of each stressor. Biplot rays radiating from the grand mean show directions of original biomarker responses in canonical space. Overlapping centroids indicate that those populations are not significantly different from one another, whereas nonoverlapping centroids indicate a difference

Metabolic Homeostasis

The most striking change in cellular biomarker pattern because of Irgarol 1051 exposure is the change in levels of some of the cnidarian porphyrin synthesis–pathway proteins. Ferrochelatase decreased significantly in both Irgarol 1051 treatments. Ferrochelatase inserts a metal ligand, usually ferrous iron (but also cobalt and zinc) into the protophorphyrin IX ring to form protoheme, the precursor of heme and other porphyrin prosthetic groups in protein complexes, such as haemoglobin and cytochrome c (Dailey *et al.* 2000). Ferrochelatase is a homodimeric, iron–sulfur protein whose activity and structure are sensitive to changes in redox state of its subcellular environment (Dailey *et al.* 2000; Marks *et al.* 1982; Marks 1985). Inhibition of this enzyme or a decrease in enzyme production can lead to an accumulation of porphyria species, specifically protoporphyrinogen (a porphyrin structure that lacks a metal group). An accumulation of porphyria species is an etiologic factor for a pathology known as *porphyria* (Thunell 2000). These porphyria species can cause immediate, direct adverse effects by producing singlet oxygens (a reactive oxygen species) from light and molecular oxygen, a significant source of oxidative stress (Thunell & Harper 2000). A decrease in ferrochelatase and therefore cytochrome species would potentially lead to abnormal conditions for during a hundred different metabolic pathways (Thunell & Harper 2000). One of these pathways is the cytochrome P450 mono-oxygenase system, which has a porphyrin (cytochrome) as an essential prosthetic group.

Protoporphyrinogen oxidase IX (PPO) is a mitochondrial enzyme that catalyses the last step in porphyrin synthesis before the insertion of the metal ligand by ferrochelatase. PPO levels significantly increased, possibly reflecting a cellular requirement for metalloporphyrins (*e.g.*, heme). Increased PPO with a decrease in ferrochelatase suggests that protoporphyrin species may be hyperaccumulating as a result of this defect in the heme-synthesis pathway (Marks 1985). Cnidarian heme oxygenase I (HO), also known as Hsp32, increased several-fold in response to Irgarol 1051 exposure. HO functions to degrade porphyrins into bilivedin, Fe, and carbon monoxide and is known to be upregulated in response to cellular stress, especially oxidative stress and toxicant exposure (Stonard *et al.* 1998; Schwartzburd 2001). Increase production of HO strongly suggests an increase in the production of broken hemin (porphyrins with the iron inserted), an increase in the production of porphyria species, or both. Canonical correlation analysis for the three cnidarian heme-metabolism proteins clearly differentiate the Irgarol 1051–exposed coral from the control treatments, providing further evidence that Irgarol 1051 exerts porphyrin-metabolic toxicity (Fig. 8). Although this is only a preliminary study, the next step would be to confirm the accumulation and types of porphyria species resulting from Irgarol 1051 exposure, which will also help determine if this herbicide inhibits other enzymes in the porphyrin synthesis pathway (*e.g.*, δ–aminolevulinic acid synthetase).

Three subfamilies of the sHsp family were examined (1) four cnidarian sHsps isoforms (*i.e.*, total sHsps22, sHsp23, and sHsp28), (2) dinoflagellate class I-II (cytosolic) sHsps, and (3) the dinoflagellate chloroplast small Hsp (class IV). The three invertebrate sHsps are confined to different cellular locations and are proposed to have different functions in protecting cellular processes during stress (Morrow *et al.* 2004). In adult organisms, these three proteins are tightly controlled and are usually only upregulated in response to dire stress conditions (Arrigo & Pauli 1998; Michaud *et al.* 1997). Induction of the invertebrate sHsp at 8 hours but not at 24 hours suggests that this pattern may be associated with exposure to light. (Irgarol toxicity is light dependent; inhibition of the *Qb* binding site may lead to the generation of reactive oxygen species resulting in an oxidative stress, thereby requiring the presence of the stabilizing and protective functionality of the sHsps. Oxidative stress could also arise as a result of the generation of singlet oxygen radicals from protoporphyrin photodynamic action (Halliwell & Gutteridge 1999). Both oxidative stress mechanisms would be absent in the absence of light, a possible explanation for the lack of sHsps induction in the 24-hour treatment. Another explanation is that the statistical differentiation is artifactual; a possibility based on the high variance levels.

The dinoflagellate class I and II sHsps localize to the algal nucleus and cytosol, are tightly regulated, are inducible by stress, and are thought to protect cytoskeletal and nuclear functions (Sun *et al.* 2002; Basha *et al.* 2004). Lack of induction of these classes of sHsps suggests that the level of stress in these locations within the dinoflagellate cell is not dire, an interpretation supported by protein metabolic condition profiles of the dinoflagellate. The chloroplast small Hsp is a unique sHsp homologue that stabilizes and localizes to photosystem II during stress (Heckathorn *et al.* 1998; 1999; Downs *et al.* 1999b, 2000). It is upregulated by factors that destabilize photosystem II efficiency by way of a photo-

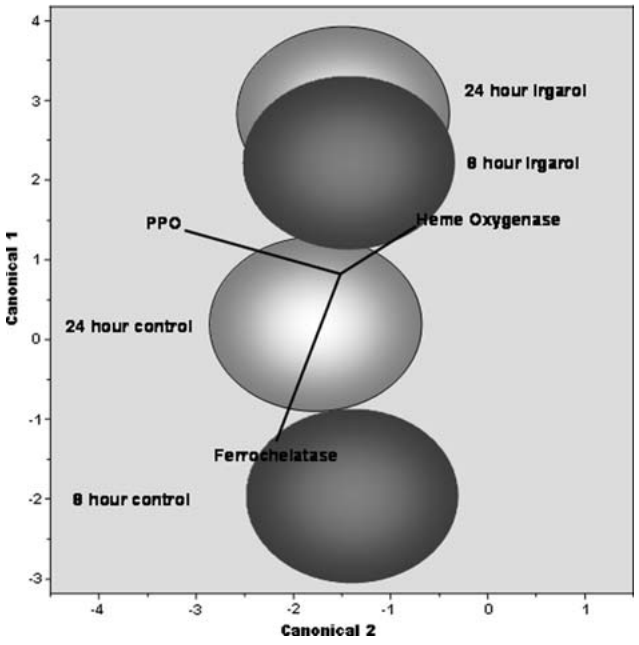

Fig. 8. Canonical centroid plot of cnidarian porphyrin metabolism biomarkers. Original variates were biomarker levels expressed as a percentage of the control value in each treatment. Circles show the 95% confidence intervals about the distribution centroid of each stressor. Biplot rays radiating from the grand mean show directions of original biomarker responses in canonical space. Overlapping centroids indicate that those populations are not significantly different from one another, whereas nonoverlapping centroids indicate a difference

oxidative mechanism; this includes factors such as heat stress, ultraviolet light and high-light stress, and PSII herbicides (Downs *et al.* 1999a). Significant accumulation of this protein in response to Irgarol 1051 exposure is consistent with both the mode of action of this herbicide as well as the function of the chloroplast sHsp (Hall *et al.* 1999; Heckathorn *et al.* 1999).

Xenobiotic Response

The original hypothesis was that Irgarol 1051 exposure would cause an induction of at least some of the CYP P450 monooxygenase enzymes. Our data show that the opposite occurred, and expression of phase I detoxification enzymes in the cnidarian were significantly *depressed* (Table 1). CYP P450-3 class immunohomologues, although playing a role in steroidogenesis, are also principal phase I detoxification enzymes for a wide variety of xenobiotics (Crampton *et al.* 1999; Ranson *et al.* 2002). CYP P450-6 class immunohomologues play a significant role in insecticide resistance in invertebrates (Liu & Scott 1998; Ranson *et al.* 2002). In mammals, atrazine is primarily metabolized by CYP P450-2 class enzymes (Hanioka *et al.* 1999), and, unfortunately, none of our antibodies against the CYP P450-2 class detected a valid target in *Madracis* (data not shown). That the level of both enzyme classes decreased suggests three plausible hypotheses: (1) Irgarol 1051 acts as a transcriptional and translational regulatory agent to inhibit production of these CYP P450 classes; (2) Irgarol 1051 acts as an irreversible inhibitor of these enzymes, thereby increasing protein degradation of these enzymes and consequently decreasing overall CYP P450 levels; or (3) Irgarol 1051 acts to inhibit production of essential ligands of the CYP P450 protein complex, thereby preventing the assembly and accumulation of these enzymes. The hypothesis that Irgarol 1051 is acting as an inhibitor of ligand production is consistent with the behaviour of other biomarkers in the other subcellular categories, notably those for metabolic homeostasis. Cytochromes are derived from porphyrins and a decrease in the amount of heme porphyrin available for cytochrome generation could influence cytochrome levels: As shown previously, ferrochelatase levels significantly decreased with Irgarol 1051 exposure, while PPO significantly increased, suggesting an inhibition of hemin production and cellular compensatory action to low hemin levels. Regardless of the mechanism, the decrease of both these CYP P450 classes suggests higher-order pathophysiologic effects: Both enzyme classes most likely play a role in steroidogenesis, consequently affecting endocrine, reproductive, membrane, and neurobehavior functions (Lewis 2004).

Levels of the phase II detoxification enzyme glutathione-s-transferase (GST) in both species were unaffected by Irgarol 1051 exposure. The cnidarian GST detected by our immunoassay is an invertebrate homologue of the highly conserved GST alpha (A1-1) that is found predominantly in the mitochondria and targets aldehyde-based toxins and toxicants, predominantly oxidative damage products such as malondialdehyde and 4-hydroxynonenal (Parkes *et al.* 1993; Ketter 2001; Raza *et al.* 2002). This GST allozyme is upregulated when oxidative stress is occurring in the mitochondria and only slightly upregulated in response to oxidative stress in the cytosol. The dinoflagellate GST is a theta-class GST homologue and is known to be upregulated in response to halogenated methanes, alkanes, and alkenes (Ketter 2001; Dixon *et al.* 2002). Triazines are known to be conjugated to glutathione by GST pi–class homologues, so it is not surprising that neither GST species were upregulated to directly aid in the xenobiotic clearance of Irgarol 1051 from the cell (Abel *et al.* 2004).

Phase III enzymes, such as the adenosine triphosphate–binding cassette family of proteins, also known as p-glycoproteins or multi-xenobiotic/multidrug resistance (MXR or MDR) proteins, export glutathione-conjugated xenobiotics from the cell (Sauna *et al.* 2001). Measurement of total MXR uses an antibody, which binds to a domain found in both host p-glycoprotein 170 (MDR1 homologue) and plant p-glycoprotein 160, that is 100% identical between the two species. These two proteins are primary MXR exporters of xenobiotics from the cell. MXR (*dinoflagellate*) is assayed by an antibody raised against a conserved domain found only on the plant MXR homologue (Martinoia *et al.* 2002). MXR (dinoflagellate) significantly increased in response to Irgarol 1051 exposure, demonstrating that the coral algal symbiont recognizes Irgarol 1051 as a xenobiotic and responds to it by clearing it from its cellular system (Table 1). Total MXR was also increased, in excess of the dinoflagellate MXR response alone (Table 1). This suggests that both species' phase III systems respond to Irgarol 1051 exposure. Increases in MXR occurred within 8 hours, suggesting rapid uptake of this herbicide by the symbiosis. Uptake and depuration kinetics of

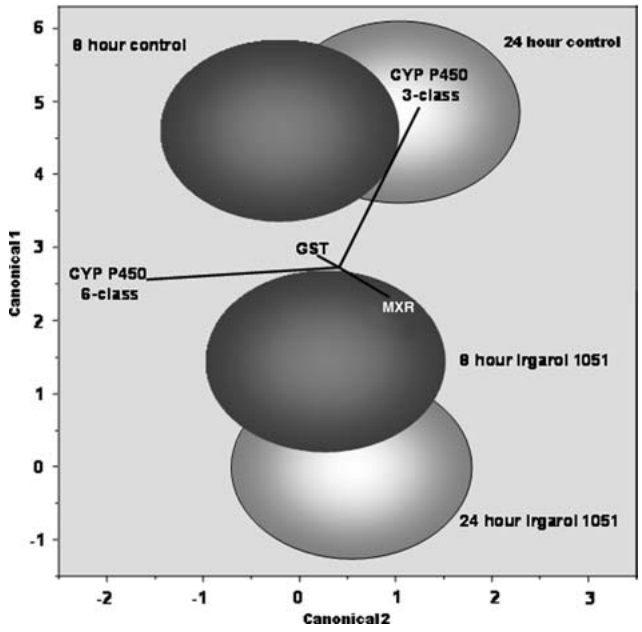

Fig. 9. Canonical centroid plot of cnidarian xenobiotic response biomarkers. Original variates were biomarker levels expressed as a percentage of the control value in each treatment. Circles show the 95% confidence intervals about the distribution centroid of each stressor. Biplot rays radiating from the grand mean show directions of original biomarker responses in canonical space. Overlapping centroids indicate that those populations are not significantly different from one another, whereas nonoverlapping centroids indicate a difference

Irgarol 1051 in corals have not as yet been directly measured; however, impacts on coral (*Seriatopora hystrix*) photosynthesis ($\Delta F/F_m$) have been detected within 15minutes of exposure to Irgarol 1051 (3 $\mu g l^{-1}$) (Jones & Kerswell 2003). At 0.3 $\mu g l^{-1}$, $\Delta F/F_m$ decreased by 30% of control values within 90 minutes of initial exposure. These data also suggest rapid uptake of this xenobiotic by the coral symbiosis. Although Irgarol 1051 is a reversible PSII inhibitor (as with other PSII-inhibiting herbicides, such as diuron and atrazine), these investigators reported relatively slow recovery (48 hours) in $\Delta F/F_m$ during depuration postexposure to 3 $\mu g l^{-1}$ Irgarol 1051. In contrast, rapid recovery (5 hours) occurred during depuration for the same coral species exposed to diuron at the same concentration.

Canonical correlation analysis of the cnidarian xenobiotic response and dinoflagellate xenobiotic response systems shows in both cases a clear distinction between control and Irgarol 1051 treatments, supporting the argument that Irgarol 1051 has an affect on cnidarian cellular physiology and that the cnidarian cell can recognize Irgarol 1051 as a xenobiotic and ''detoxify'' the *s*-triazine (Fig. 9).

Conclusion

We assessed cellular protein expression biomarkers of protein metabolic condition, oxidative damage and response, and metabolic homeostasis and xenobiotic responses in both host (cnidarian) and dinoflagellate (endosymbiotic algae) of the branching coral *Madracis mirabilis* exposed to an initial nominal concentration of 10 $\mu g\ l^{-1}$ of the antifouling herbicide Irgarol 1051 during 24 hours. We intentionally selected this concentration to allow an assessment of potential toxicity mechanisms associated with Irgarol 1051 exposure and have made no attempt to measure the uptake of Irgarol 1051 by corals during the experiment, nor have we made any assessment of dose response. We have not assessed responses associated with the more environmentally realistic scenario of chronic low-level exposure at concentrations of 0.01 to 1 $\mu g\ l^{-1}$ or the potential influences of temperature and incident irradiance. These studies should be conducted. This preliminary data, however, provide an insight into mechanisms of toxicity (notably metabolic toxicity) of Irgarol 1051 to the coral symbiosis. The approach of cellular diagnostics shows that end points that assess photosynthetic inhibition alone (Owen *et al.* 2002, 2003; Jones & Kershwell 2003), although important, are insufficient to provide a comprehensive assessment of the sublethal hazard posed by this herbicide, a common contaminant, to corals.

In particular, the data lead us to hypothesise that Irgarol 1051 impacts porphyrin synthesis within the coral symbiosis. Secondary effects resulting from disruption of porphyrin synthesis may include impact on synthesis of important biosynthetic enzymes, such as those within the cytochrome P450 system and related higher-order pathophysiologic effects, including steroidogenesis and reproductive impairment. These should be studied in more detail for both Irgarol 1051 and other methylthio-substituted triazines, such as ametryn and prometryn, in both coral and other invertebrate (and indeed vertebrate) species.

Irgarol 1051 exposure also causes oxidative stress within the symbiosis and compromises oxidative defence capacity (*e.g.*, through decrease in catalase). Antioxidant capacity is important for corals containing photosynthetic dinoflagellate, particularly in high irradiance, shallow water environments, while oxidative stress within the symbiosis is an important determinant of the coral bleaching process (Brown *et al.* 2002a, b; Downs *et al.* 2002). Compromising the ability of the symbiosis to decrease cellular free radical burden, while simultaneously increasing free radical production, suggests a potential role for this herbicide in terms of influencing coral susceptibility to the bleaching phenomenon.

Acknowledgments. This work was funded by EnVirtue Biotechnologies, Inc, and the Department of Environmental Protection, Bermuda Government. We thank Richard Owen and Lucy Buxton for their help in setting up the experiments in Bermuda. We also thank the two anonymous reviewers for their careful editing and improvements to the manuscript.

References

Abel EL, Opp SM, Verlinde CL, Bammler TK, Eaton DL (2004), Characterization of atrazine biotransformation by human and murine glutathione s-transferases. Toxicol Sci 80:230–238

Adams J (2004) The development of proteasome inhibitors as anticancer drugs. Cancer Cell 5:417–421

Arrigo A, Pauli D (1998) Characterization of hsp27 and three immunologically related polypeptides during Drosophila development. Exp Cell Res 175:169–183

Basha E, Lee GJ, Demeler B, Vierling E (2004) Chaperone activity of cytosolic small heat shock proteins from wheat. Eur J Biochem 271:1426–1436

Basheer C, Tan KS, Lee HK (2002) Organotin and Irgarol 1051 contamination in Singapore coastal waters. Mar Poll Bull 44:697–703

Berleth ES, Pickart CM (1996) Mechanism of ubiquitin conjugating enzyme E2-230K: Catalysis involving thiol relay? Biochemistry 35:1664–1671

Bonassi S, Au WW (2002) Biomarkers in molecular epidemiology studies for health risk prediction. Mutat Res 511:73–86

Bonassi S, Neri M, Puntoni R (2001) Validation of biomarkers as early predictors of disease. Mutat Res 480–481:349–358

Brown B, Downs CA, Dunne RP, Gibb SW (2002a) Exploring the basis of thermotolerance in the reef coral *Goniastrea aspera*. Mar Ecol Prog Ser 242:119–129

Brown BA, Downs CA, Dunne RP, Gibb SW (2002b) Preliminary evidence for tissue retraction as a factor in photoprotection of corals incapable of xanthophyll cycling. J Exp Mar Biol Ecol 277:129–144

Chelikani P, Fita I, Loewen PC (2004) Diversity of structures and properties among catalases. Cell Mol Life Sci 61:192–208

Crampton AL, Baxter GD, Barker SC (1999) A new family of cytochrome P450 genes (CYP41) from the cattle tick, Boophilus microplus. Biochem Mol Biol 29:829–834

Crowther JR (2001) The ELISA guidebook. Totowa, NJ, Humana

Dahl B, Blanck H (1996) Toxic effects of the antifouling agent Irgarol 1051 on periphyton communities in coastal microcosms. Mar Pollut Bull 32:342–350

Dailey HA, Dailey TA, Wu C-K, Medlock AE, Wang K-F, Rose JP et al. (2000) Ferrochelatase at the millennium: Structures, mechanisms and [2Fe-2S] clusters. Cell Mol Life Sci 57:1909–1926

Ding Q, Dimayuga E, Martin S, Bruce-Keller AJ, Nukala V, Cuervo AM et al. (2003) Characterization of chronic low-level proteasome inhibition on neural homeostasis. Neurochemistry 86:489–497

Dixon DP, Lapthorn A, Edwards R (2002) Plant glutathione transferases. Genome Biol 3:1–10

Downs CA (2005) Cellular diagnostics and its application to aquatic and marine toxicology. In: Ostrander G (ed) Techniques in aquatic toxicology. Volume 2. CRC Press, Boca Raton, FL, pp 181–207

Downs CA, Fauth JE, Halas JC, Dustan P, Bemiss J, Woodley CM (2002) Oxidative stress and seasonal coral bleaching. Free Radic Biol Med 33:533–543

Downs CA, Mueller E, Phillips S, Fauth JE, Woodley CM (2000) A molecular biomarker system for assessing the health of coral during heat stress. Mar Biotechnol 2:533–544

Downs CA, Ryan SL, Heckathorn SA (1999a) The chloroplast small heat-shock protein: Evidence for a general role in protecting photosystem II against oxidative stress and photoinhibition. J Plant Physiol 155:488–496

Downs CA, Coleman JS, Heckathorn SA (1999b) The chloroplast 22-kDa heat-shock protein: A lumenal protein that associates with the oxygen evolving complex and protects photosystem II during heat stress. J. Plant Physiol 155:477–487

Guach HGJ (1985) Multivariate analysis in community ecology. Cambridge University Press, New York, NY

Ghosh S, Gepstein S, Heikkila JJ, Dumbroff BG (1988) Use of a scanning densitometer or an ELISA plate reader for measurement of nanogram amounts of protein in crude extracts from biological tissue. Anal Biochem 169:227–233

Haeger-Aronsen B (1964) Experimental disturbance of porphyrin metabolism and of liver catalase activity in guinea pigs and rabbits. Acta Pharmacol Toxicol 21:105–115

Hall LW Jr, Giddings JM, Solomon KR, Balcomb R (1999) An ecological risk assessment for the use of Irgarol 1051 as an algaecide for antifoulant paints. Crit Rev Toxicol 29:367–437

Hall LW Jr, Killen WD, Gardinali PR (2004) Occurrence of Irgarol 1051 and its major metabolite in Maryland waters of Chesapeake Bay. Mar Pollut Bull 48:554–562

Halliwell B, Gutteridge JMC (1999) Free radicals in biology and medicine. 3rd ed. Oxford Science, Oxford, UK

Hanioka N, Jinno H, Tanaka-Kagawa T, Nishimura T, Ando M (1999) In vitro metabolism of chlorotriazines: Characterization of simazine, atrazine, and propazine metabolism using liver microsomes from rats treated with various cytochrome P450 inducers. Toxicol Appl Pharmacol 156:195–205

Heckathorn SA, Downs CA, Coleman JS (1999) Small heat-shock proteins protect electron transport in chloroplasts and mitochondria during stress. Am Zool 39:865–876

Heckathorn SA, Downs CA, Sharkey TD, Coleman JS (1998) The small methionine-rich chloroplast heat-shock protein protects photosystem II electron transport during heat stress. Plant Physiol 116:439–444

Hershko A, Heller H, Eytan E, Reiss Y (1986) The protein substrate binding site of the ubiquitin-protein ligase system. J Biol Chem 261:11992–11999

Jones RJ, Kerswell AP (2003) Phytotoxicity evaluation of Photosystem II (PSII) herbicides on scleratinian coral. Mar Ecol Prog Ser 261:149–159

Ketter B (2001) A bird's eye view of the glutathione transferase field. Chem Biol Interact 138:27–42

Konstantinou IK, Albanis TA (2004) Worldwide occurrence and effects of antifouling paint booster biocides in the aquatic environment: a review. Environ Int 30:235–248

Lewis DF (2004) 57 varieties: The human cytochromes P450. Pharmacogenomics 5:305–318

Lledias F, Rangel P, Hansberg W (1998) Oxidation of catalase by singlet oxygen. J Biol Chem 273:10630–10637

Liu N, Scott JG (1998) Increased transcription of CYP6D1 causes cytochrome P450-mediated insecticide resistance in house fly. Insect Biochem Mol Biol 28:531–535

Marks GS, Zelt DT, Cole SPC (1982) Alteration in the heme biosynthetic pathway as an index of exposure to toxins. Can J Physiol Pharmacol 60:1017–1026

Marks GS (1985) exposure to toxic agents: The heme biosynthetic pathway and the hemoproteins as indicators. Crit Rev Toxicol 15:151–179

Martinoia E, Klein M, Geisler M, Bovet L, Forestier C, Kolukisaoglu U et al. (2002) Multifunctionality of plant ABC transporters—More than just detoxifiers. Planta 214:345–355

Michaud S, Marin R, Tanguay RR (1997) Regulation of heat shock gene induction and expression during Drosophila development. Cell Mol Life Sci 53:104–113

Morrow G, Samson M, Michaud S, Tanguay RM (2004) Overexpression of the small mitochondrial Hsp22 extends Drosophila life span and increases resistance to oxidative stress. FASEB J 18:598–589

Owen R, Knap AH, Toaspern M, Carbery K (2002) Inhibition of coral photosynthesis by the antifouling herbicide Irgarol 1051. Mar Pollut Bull 44:623–632

Owen R, Knap AH, Ostrander N, Carbery K (2003) Comparative acute toxicity of herbicides to photosynthesis of coral dinoflagellate. Bull Environ Contam Toxicol 70:541–548

Parkes TL, Hilliker AJ, Phillips JP (1993) Genetic and biochemical analysis of glutathione-s-transferase in the oxygen defense system of *Drosophila melanogaste*r. Genome 36:1007–1014

Perera FP (2000) Molecular epidemiology: On the pathway to prevention? J Natl Cancer Inst 92:602–612

Ranson H, Claudianos C, Ortelli F, Abgrall C, Hemingway J, Sharakhova MV et al. (2002) Evolution of supergene families associated with insecticide resistance. Science 298:179–181

Raza H, Robin M, Fang J, Avadhani NG (2002) Multiple isoforms of mitochondrial glutathione-s-transferases and their differential induction under oxidative stress. Biochem J 366:45–55

Raynor C (1999) Advances in sulfur chemistry. Volume 2. Elsevier Science, Oxford, UK

Readman JW, Wee Knong LL, Grondin D, Barocci J, Villeneuve LP, Mee LD (1993) Coastal water contamination from a triazine herbicide used in antifouling paints. Environ Sci Technol 17:553–556

Sauna ZE, Smith MM, Muller M, Kerr KM, Ambudkar SV (2001) The mechanism of action of multidrug-resistance-linked P-glycoprotein. J Bioenerg Biomembr 33:481–491

Schwartzburd PM (2001) Self-cytoprotection against stress: Feedback regulation of heme dependent metabolism. Cell Stress Chaperones 6:1–5

Shimizu N, Kobayaski K, Hayashi K (1984) The reaction of superoxide radical with catalase: Mechanism of the inhibition of catalase by superoxide. J Biol Chem 259:4414–4418

Sokal RR, Rohlf FJ (1995) Biometry. Freeman, New York, NY

Stonard MD, Poli G, Matteis FS (1998) Stimulation of liver heme oxygenasein hexachlorobenzene-induced hepatic porphyria. Arch Toxicol 72:355–361

Sun W, Van Montagu M, Verbruggen N (2002) Small heat shock proteins and stress tolerance in plants. Biochim Biophys Acta 21577:1–9

Teschke R., Boelsen, Landmann H, Goerz G (1983) Effect of hexachlorobenzene on the activities of hepatic alcohol metabolizing enzymes. Biochem Pharmacol 32:1745–1751

Thomas KV (2001) The environmental fate and behaviour of antifouling paint—Booster biocides: A review. Biofouling 17:73–86

Thunell S (2000) Porphyrins, porphyrin metabolism and porphyries. I. Update Scand J Clin Lab Invest 60:509–540

Thunell S, Harper P (2000) Porphyrins, porphyrin metabolism, porphyries. III. Diagnosis, care, and monitoring in porphyria cutanea tarda—Suggestions for a handling programme. Scand J Clin Lab Invest 60:561–580

Wu G, Wilen RW, Robertson AJ, Gusta LV (1999) Isolation, chromosomal localization, and differential expression of mitochondrial manganese superoxide dismutase and chloroplastic copper/zinc superoxide dismutase genes in wheat. Plant Physiol 120:513–520